Fluctuations, Correlations, and Small-Angle Neutron Scattering from End-Linked Gaussian Chains in Regular Bimodal Networks

A. Kloczkowski* and J. E. Mark

Department of Chemistry and Polymer Research Center, University of Cincinnati, Cincinnati, Ohio 45221-0172

B. Erman

Polymer Research Center, School of Engineering, Bogazici University, Bebek 80815, Istanbul, Turkey

Received November 14, 1990

ABSTRACT: Fluctuations of junctions and correlations between fluctuations of junctions connected by short and long chains have been calculated for regular bimodal Gaussian phantom networks with treelike topology as a function of the ratio ξ of lengths of short and long chains. The regularity of the network is preserved by the requirement that each junction of the network is connected with a constant number ϕ_S of short chains and a constant number ϕ_L of long chains, so that the functionality of the network is $\phi = \phi_S + \phi_L$. Networks of this type have been recently synthesized by Sharaf and Mark. The fluctuations of mean-square end-to-end distances for short and long chains and small-angle neutron scattering factors for scattering from labeled end-linked short and long chains in regular bimodal networks have been studied.

Introduction

The theory of phantom networks, introduced by James and Guth[1,2] and later developed by various authors,[3-9] leads to expressions for fluctuations of chain dimensions, of junctions, and of paths separated by several junctions. These theories assume that chains are connected by cross-links to form a network with a small set of fixed points at the bounding surface of the network. All chains and junctions inside the polymer fluctuate around their well-defined mean positions. It is assumed that fluctuations of junctions and chains are strain independent, while all average positions transform affinely with applied strain. Chains are assumed to be Gaussian. Not only is their distribution of contour lengths taken to be unimodal, it is assumed to be single valued (all chains having the same length). Bimodal Gaussian phantom networks have been treated only recently in a very comprehensive manner by Higgs and Ball.[10] The latter gives the fluctuations of junctions as the solution of a nonlinear integral equation and is exact within the premises of the phantom network structure. A mean-field approximate solution is also provided that applies to bimodal networks when the difference in the lengths of the short and the long chains is not large. The theory of Higgs and Ball is derived for a random bimodal network where each junction may contain various combinations of short and long chains. The treatment of Higgs and Ball describes essentially all aspects of fluctuations in random bimodal networks.

In the present study, we present an exact analysis of networks with a regular structure, i.e., with a fixed number ϕ_S of short and a fixed number ϕ_L of long chains at every junction. Both the short chains and long chains are monodisperse in their separate length distributions. The study is motivated essentially by the recent possibility of synthesizing such regular networks[11] by using polysulfidic cross-linking agents, which themselves act as short chains in a bimodal network with trifunctional junctions. One may visualize several different types of networks with regular structure that may be obtained by well-controlled preparation techniques. The present study outlines the basic features of regular trifunctional and tetrafunctional networks with Gaussian short and long chains.

Theory of Phantom Networks

The distribution $W(r)$ of the end-to-end vector $\mathbf{r}$ of the network chain in the undeformed state is given by

$$W(r) = \left(\frac{3}{2\pi\langle r^2\rangle_0}\right)^{3/2} \exp(-3r^2/2\langle r^2\rangle_0) \qquad (1)$$

where $\langle r^2\rangle_0$ is the mean-square end-to-end vector of chains in the undeformed state. In the unimodal (monodisperse) network, all chains have the same length and distribution of end-to-end vectors $W(r)$ with one mean-square end-to-end distance $\langle r^2\rangle_0$. In the bimodal network, both short chains and long chains have different Gaussian distributions with mean-square end-to-end distance $\langle r_S^2\rangle_0$ for short chains and $\langle r_L^2\rangle_0$ for long ones. In polydisperse networks, there is a distribution of mean-square end-to-end vectors corresponding to chains of different contour lengths.

The configuration partition function Z_N for the phantom network is a product of configuration functions for individual chains

$$Z_N = C\prod_{i<j} \exp(-3r_{ij}^2/2\langle r_{ij}^2\rangle_0) \qquad (2)$$

since, due to the phantomlike nature of the network, intermolecular contributions to the configurations partition function are neglected. Here C is a constant and the product includes all pairs of junctions joined by a chain.

Equation 2 may be written as follows[7-9]

$$Z_N = C\exp(-\sum_i\sum_j \gamma_{ij}\mathbf{R}_i\cdot\mathbf{R}_j) \equiv C\exp(-\{\mathbf{R}\}^T\Gamma\{\mathbf{R}\}) \qquad (3)$$

where $\mathbf{R}_i$ and $\mathbf{R}_j$ are position vectors of junctions i and j ($r_{ij} = |\mathbf{R}_i - \mathbf{R}_j|$) and $\{\mathbf{R}\}$ is a column vector formed by position vectors of all junctions. The off-diagonal elements γ_{ij} ($i \neq j$) of the matrix Γ are defined as

$$\gamma_{ij} = \begin{cases} -\dfrac{3}{2\langle r_{ij}^2\rangle_0} & \text{if junctions } i \text{ and } j \text{ are connected} \\ 0 & \text{otherwise} \end{cases} \qquad (4)$$

and the diagonal elements of Γ are sums of its off-diagonal

0024-9297/91/2224-3266$02.50/0

elements in a given row (column) taken with the negative sign

$$\gamma_{ii} = -\sum_{j \neq i} \gamma_{ij} = -\sum_{j \neq i} \gamma_{ji} \tag{5}$$

The fluctuation $\Delta\mathbf{R}_i$ of the ith junction is

$$\Delta\mathbf{R}_i = \mathbf{R}_i - \bar{\mathbf{R}}_i \tag{6}$$

where $\mathbf{R}_i$ is the instantaneous position vector of the junction and $\bar{\mathbf{R}}_i$ its mean-time-averaged position.

The correlation of fluctuations of two junctions i and j obtained from eq 3 is[7-9]

$$\langle \Delta\mathbf{R}_i \cdot \Delta\mathbf{R}_j \rangle = \frac{\int \Delta\mathbf{R}_i \cdot \Delta\mathbf{R}_j \exp[-\{\Delta\mathbf{R}\}^T \Gamma \{\Delta\mathbf{R}\}] \, d\{\Delta\mathbf{R}\}}{\int \exp[-\{\Delta\mathbf{R}\}^T \Gamma \{\Delta\mathbf{R}\}] \, d\{\Delta\mathbf{R}\}} = \frac{3}{2}(\Gamma^{-1})_{ij} \tag{7}$$

Here $\{\Delta\mathbf{R}\}$ is a column vector formed by fluctuation vectors of all junctions, and $(\Gamma^{-1})_{ij}$ is the i–jth element of the inverse matrix Γ^{-1}. Equation 7 holds for all junctions joined directly by a chain or separated by several other junctions. In the special case where $i = j$, eq 7 gives for the mean-square fluctuations of the ith junction in the network

$$\langle (\Delta R_i)^2 \rangle = \frac{3}{2}(\Gamma^{-1})_{ii} \tag{8}$$

The mean-square fluctuations of the distances $r_{ij} = |\mathbf{R}_i - \mathbf{R}_j|$ between junctions i and j are

$$\langle (\Delta r_{ij})^2 \rangle = \langle (\Delta\mathbf{R}_i - \Delta\mathbf{R}_j)^2 \rangle = \langle (\Delta R_i)^2 \rangle + \langle (\Delta R_j)^2 \rangle - 2\langle (\Delta\mathbf{R}_i \cdot \Delta\mathbf{R}_j) \rangle = \frac{3}{2}[(\Gamma^{-1})_{ii} + (\Gamma^{-1})_{jj} - 2(\Gamma^{-1})_{ij}] \tag{9}$$

The connectivity matrix Γ is known as the Kirchhoff or valency-adjacency matrix in graph theory.[4] Its form depends on the topological structure and the connectivity of the network. The inverse matrix Γ^{-1} fully determines the fluctuations and correlations of all chains and junctions in the phantom network and the scattering form factor for the small-angle neutron scattering (SANS) from the network. The inverse matrix Γ^{-1} for a unimodal (monodisperse) Gaussian phantom network with the topology of the infinite, symmetrically grown tree has been calculated recently.[9] This result enabled us to calculate chain dimensions, fluctuations, and SANS from labeled cross-linked paths in unimodal (monodisperse) phantom networks. The present paper extends some of these results to bimodal networks.

Regular Bimodal Networks

We will study regular bimodal networks with the topology of an infinite, symmetrically grown tree. An example of such a network is shown in Figure 1. It is assumed that all junctions have the same functionality ϕ and each junction contains the same number ϕ_L of long and ϕ_S of short chains, i.e.

$$\phi = \phi_L + \phi_S \tag{10}$$

It means that all junctions in the regular bimodal network have the same structure. For example, the regular trifunctional bimodal network shown in Figure 1 has $\phi_L = 2$ and $\phi_S = 1$. All short chains have the same length, and all long chains have the same length. The connectivity matrix Γ for a regular trifunctional bimodal network shown in Figure 1 is given in eq 11 below with diagonal elements $a = -2\phi_L - \phi_S$. The network grows symmetrically from the central chain (short chain in Figure 1) between junctions 1 and 2. These two junctions constitute the first tier of junctions, and the second tier consists of junctions

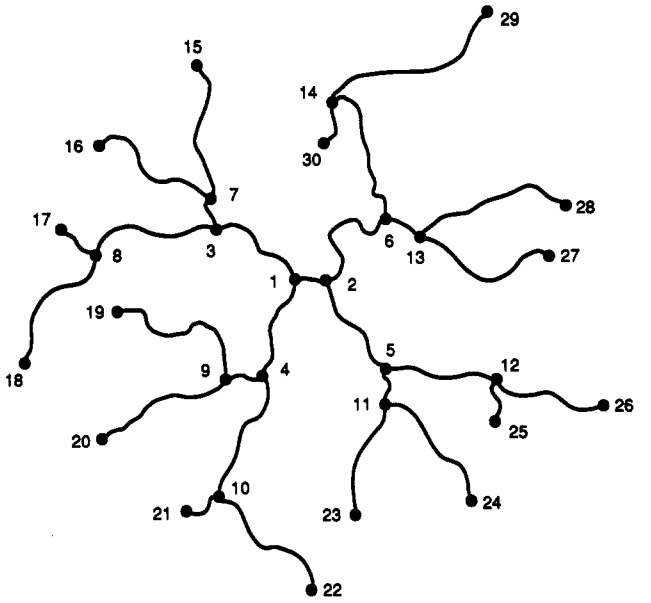

Figure 1. Regular bimodal trifunctional ($\phi = 3$) network composed of four tiers. Each junction in the network is connected with one short chain ($\phi_S = 1$) and two long chains ($\phi_L = 2$).

numbered from 3 to 6. The third tier is composed of junctions 7–14, and the fourth tier contains junctions 15–30. It is assumed that the network grows in this way to

$\Gamma =$

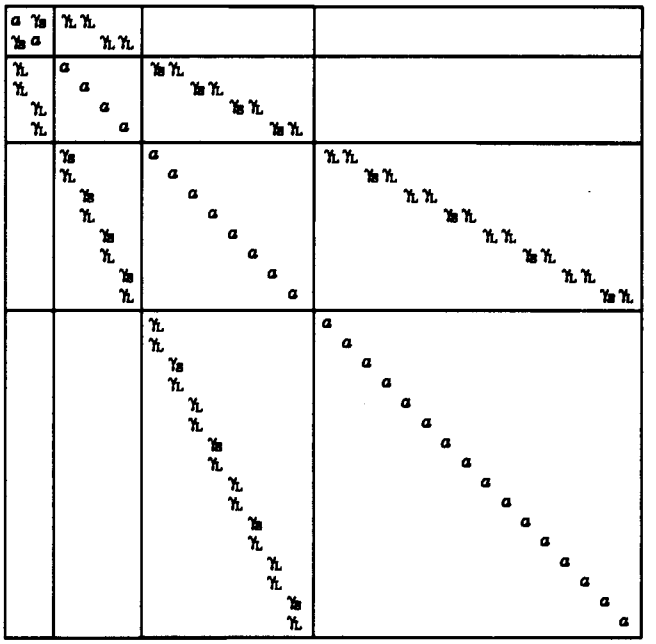

(11)

infinity and that the junctions in the last tier are connected with fixed points in such a way that the numbers ϕ_L and ϕ_S of long and short chains for the junctions in the last tier are the same as for other junctions within the network. The numbering scheme for junctions in the network shown in Figure 1 gives a highly regular form for the connectivity matrix Γ. The matrix, shown in eq 11, is partitioned for easy reference into submatrices corresponding to different tiers and grows to the right and downward as the size of the network increases. The ith row or column of the connectivity matrix Γ is associated with the ith junction. The generalization of matrix Γ to a regular bimodal network with arbitrary functionality $\phi = \phi_L + \phi_S$ ($\phi > 2$), where ϕ_L and ϕ_S are integer numbers constant for all junctions in the network, is straightforward. The special

case $\phi_L = 0$ or $\phi_S = 0$ corresponds to a unimodal network. If the central chain constituting the first tier around which the symmetrical tree is growing is a short one, then the second tier contains $N_2^S = 2(\phi_S - 1)$ short chains and $N_2^L = 2\phi_L$ long chains, and thus the total number of chains in the second tier is $N_2 = 2(\phi - 1)$. The third tier contains $N_3^S = 2(\phi_S - 1)^2 + 2\phi_S\phi_L$ short chains and $N_3^L = 2\phi_L(\phi_L - 1) + 2(\phi_S - 1)\phi_L$ long ones, and thus the total number of chains in the third tier is $N_3 = 2(\phi - 1)^2$. Generally, if the network is grown around a short chain and the number of short and long chains in the $(k - 1)$th tier is N_{k-1}^S and N_{k-1}^L, respectively, then the corresponding number of short and long chains in the kth tier is

$$N_k^S = (\phi_S - 1)N_{k-1}^S + \phi_S N_{k-1}^L$$

$$N_k^L = (\phi_L - 1)N_{k-1}^L + \phi_L N_{k-1}^S \quad (12)$$

and the total number of chains in the kth tier is

$$N_k = N_k^L + N_k^S = 2(\phi - 1)^{k-1} \quad (13)$$

When $k = 1$, $N_1^S = 2$ and $N_1^L = 0$. These values of N_1^S and N_1^L correspond to the number of junctions joined by a central chain and only in this case does the number of junctions and tiers differ. The kth tier is associated with the kth diagonal submatrix of Γ of order $N_k \times N_k$. For a given junction in the kth tier, a single entry γ_S (or γ_L) to the left of the diagonal corresponds to a connection by a short (or long) chain with a junction in the $(k - 1)$th tier and the entries γ_S and γ_L on the right of the diagonal ($\phi - 1$ in total number) to a connection by short and long chains with $\phi - 1$ junctions in the $(k + 1)$th tier. All diagonal elements of Γ are

$$\gamma_{ii} = -\phi_S\gamma_S - \phi_L\gamma_L \quad (1 \le i \le N) \quad (14)$$

where N is the total number of free junctions in the network composed of t tiers

$$N = 2\frac{(\phi - 1)^t - 1}{\phi - 2} \quad (15)$$

To diagonalize the matrix Γ, we use the method of eliminating elements in the upper right half of the matrix, used previously for unimodal (monodisperse) networks.[9] Let us assume that the network has t tiers. First we multiply the last N_t rows [given by eq 13] in the connectivity matrix Γ by either

$$\gamma_S/(\phi_S\gamma_S + \phi_L\gamma_L) \quad (16)$$

if there are γ_S entries in the corresponding columns on the right of the diagonal, or by

$$\gamma_L/(\phi_S\gamma_S + \phi_L\gamma_L) \quad (17)$$

if there are γ_L entries in their corresponding columns and then add them to the preceding N_{t-1} rows such that γ_S and γ_L elements on the right of the diagonal vanish. This changes the diagonal elements of the submatrix corresponding to the $(t - 1)$th tier from

$$a_1 = b_1 = -\phi_S\gamma_S - \phi_L\gamma_L \quad (18)$$

to either

$$a_2 = -\phi_S\gamma_S - \phi_L\gamma_L - \frac{(\phi_L - 1)\gamma_L^2}{a_1} - \frac{\phi_S\gamma_S^2}{b_1} \quad (19a)$$

or

$$b_2 = -\phi_S\gamma_S - \phi_L\gamma_L - \frac{\phi_L\gamma_L^2}{a_1} - \frac{(\phi_S - 1)\gamma_S^2}{b_1} \quad (19b)$$

In the next step, we multiply the N_{t-1} rows of Γ corresponding to the $(t - 1)$th tier by either $-\gamma_S/a_2$ (or $-\gamma_S/b_2$) if there are γ_S entries and the diagonal elements are a_2 (or b_2) in the corresponding columns on the right of the diagonal or by $-\gamma_L/a_2$ (or $-\gamma_L/b_2$) if there are γ_L entries in the corresponding columns to the right of the diagonal and the diagonal elements are a_2 (or b_2). This changes the diagonal elements of the submatrix corresponding to the $(t - 2)$th tier to either

$$a_3 = -\phi_S\gamma_S - \phi_L\gamma_L - \frac{(\phi_L - 1)\gamma_L^2}{a_2} - \frac{\phi_S\gamma_S^2}{b_2} \quad (20a)$$

or

$$b_3 = -\phi_S\gamma_S - \phi_L\gamma_L - \frac{\phi_L\gamma_L^2}{a_2} - \frac{(\phi_S - 1)\gamma_S^2}{b_2} \quad (20b)$$

Continuation of this process leads to the matrix whose diagonal elements a_{k+1}, b_{k+1} corresponding to the $(t - k)$th tier are related to the diagonal elements a_k, b_k corresponding to the $(t - k + 1)$th tier by the double-recurrence relation

$$a_{k+1} = -\phi_S\gamma_S - \phi_L\gamma_L - \frac{(\phi_L - 1)\gamma_L^2}{a_k} - \frac{\phi_S\gamma_S^2}{b_k} \quad (21a)$$

$$b_{k+1} = -\phi_S\gamma_S - \phi_L\gamma_L - \frac{\phi_L\gamma_L^2}{a_k} - \frac{(\phi_S - 1)\gamma_S^2}{b_k} \quad (21b)$$

Finally, if the central chain cross-linking the first tier is a long one, then the diagonal submatrix corresponding to the first tier becomes

$$\Gamma_1 = \begin{bmatrix} a_t & \gamma_L \\ \gamma_L & a_t \end{bmatrix} \quad (22)$$

If the central chain constituting the first tier of the network is a short one, then the diagonal submatrix corresponding to the first tier is

$$\Gamma_1 = \begin{bmatrix} b_t & \gamma_S \\ \gamma_S & b_t \end{bmatrix} \quad (23)$$

The elements of the inverse matrix Γ^{-1} corresponding to fluctuations of junctions 1 and 2 in the first tier and to the correlations between fluctuations of these junctions are

$$\Gamma_1^{-1} = \begin{bmatrix} \frac{a_t}{a_t^2 - \gamma_L^2} & \frac{-\gamma_L}{a_t^2 - \gamma_L^2} \\ \frac{-\gamma_L}{a_t^2 - \gamma_L^2} & \frac{a_t}{a_t^2 - \gamma_L^2} \end{bmatrix} \quad (24)$$

if the chain between junctions 1 and 2 is a long one, and

$$\Gamma_1^{-1} = \begin{bmatrix} \frac{b_t}{b_t^2 - \gamma_S^2} & \frac{-\gamma_S}{b_t^2 - \gamma_S^2} \\ \frac{-\gamma_S}{b_t^2 - \gamma_S^2} & \frac{b_t}{b_t^2 - \gamma_S^2} \end{bmatrix} \quad (25)$$

if the chain between junctions 1 and 2 is a short one. The calculation of fluctuation of junctions and the correlations between them requires the solutions a_t, b_t (for $t \to \infty$) of the double-recurrence relations (eqs 21a and 21b) with

the initial condition given by eq 18. In the special case where $\phi_S = 0$ (or $\phi_L = 0$), the double-recurrence formula reduces to the single recursion

$$a_1 = -\phi\gamma \tag{26}$$

$$a_{k+1} = -\phi\gamma - \frac{(\phi-1)\gamma}{a_k} \tag{27}$$

with the known solution

$$a_k = -\frac{(\phi-1)^{k+1}-1}{(\phi-1)^k-1}\gamma \tag{28}$$

which, in the limit $k \to \infty$, becomes

$$\lim_{k\to\infty} a_k = -(\phi-1)\gamma = \frac{3}{2\langle r^2\rangle_0}(\phi-1) \tag{29}$$

Introducing the notation

$$A_k = -a_k/\gamma_L \tag{30}$$

$$B_k = -b_k/\gamma_L \tag{31}$$

and denoting the ratio of the contour lengths of the short chains to the long ones by ξ ($0 < \xi < 1$)

$$\gamma_L/\gamma_S = \langle r_S^2\rangle_0/\langle r_L^2\rangle_0 = \xi \tag{32}$$

permits the double-recursion formula to be written as

$$A_1 = B_1 = \phi_L + \phi_S/\xi \tag{33}$$

and

$$A_{k+1} = \phi_L + \phi_S/\xi - \frac{\phi_L - 1}{A_k} - \frac{\phi_S}{\xi^2 B_k} \tag{34a}$$

$$B_{k+1} = \phi_L + \phi_S/\xi - \frac{\phi_L}{A_k} - \frac{\phi_S - 1}{\xi^2 B_k} \tag{34b}$$

The limiting values of the coefficients $A = \lim_{k\to\infty} A_k$ and $B = \lim_{k\to\infty} B_k$ to which the double-recursion formula converges are given by the set of two algebraic equations

$$A = \phi_L + \phi_S/\xi - \frac{\phi_L - 1}{A} - \frac{\phi_S}{\xi^2 B} \tag{35a}$$

$$B = \phi_L + \phi_S/\xi - \frac{\phi_L}{A} - \frac{\phi_S - 1}{\xi^2 B} \tag{35b}$$

This is equivalent to the set of equations

$$A^2B - AB^2 - B + A/\xi^2 = 0 \tag{36a}$$

$$(\phi_L + \phi_S/\xi)AB - \phi_L B - (\phi_S - 1)A/\xi^2 - AB^2 = 0 \tag{36b}$$

From eq 36a, it follows that

$$A = \frac{B^2 - \xi^{-2} + \sqrt{(B^2-\xi^{-2})^2 + 4B^2}}{2B} \tag{37}$$

because the second root, with a negative sign, is unphysical. Substituting eq 37 into eq 36b and performing the required algebra, we obtain the quartic equation for B

$$B^4(1-\phi_L) + B^3[(\xi^{-1}\phi_S + \phi_L)(\phi_L - 2)] + B^2\{\xi^{-2}[(\phi_S - 1)(2-\phi_L) + \phi_S^2 + \phi_L] + 2\phi_L\phi_S\xi^{-1}\} + B[-\xi^{-3}(\phi_L + 2\phi_S - 2)\phi_S - \xi^{-2}\phi_L(\phi_L + 2\phi_S - 2)] + \xi^{-4}(\phi_S - 1)(\phi_L + \phi_S - 1) = 0 \tag{38}$$

Since one of the roots of eq 38 is $B = \xi^{-1}$, the quartic equation may be reduced to the cubic one

$$B^3(1-\phi_L) + B^2[\xi^{-1}(\phi_S\phi_L - 2\phi_S - \phi_L + 1) + \phi_L(\phi_L - 2)] + B[\xi^{-2}(\phi_S^2 + \phi_L - 1) + \xi^{-1}(2\phi_S\phi_L + \phi_L^2 - 2\phi_L)] - \xi^{-3}(\phi_S - 1)(\phi_S + \phi_L - 1) = 0 \tag{39}$$

In the special case when $\xi = 1$, i.e., when the bimodal network reduces to the unimodal one, one of the roots of the cubic equation (eq 39) becomes $\phi_S + \phi_L - 1 = \phi - 1$. The remaining two roots are unphysical. It is not possible to obtain the solution of eq 39 in a compact form. The Cardano formulas are too lengthy for practical use. Generally we have three roots, and the physical one is the root that gives $\phi - 1$ in the limit $\xi \to 1$. Therefore, from the practical point of view, it is easier to solve the double-recursion equation (eq 35) numerically, rather than solving the cubic equation and then analyzing to determine which of the three roots is the proper one. The double-recursion formula converges very quickly, and after less than 10 iterations, one may obtain the result to the desired accuracy. It is, however, very interesting that even for such a simple model of a bimodal network the solution cannot be written in a simple form, as was possible for unimodal networks. In the following section, we study the resulting fluctuations of chains and junctions in a bimodal network and the correlations between junctions connected by a single short or long chain.

Fluctuations in Regular Bimodal Networks

Fluctuations $\langle(\Delta R_i)^2\rangle$ of the ith junction in the network are given by eq 8, i.e., by the ith diagonal element of the inverse matrix Γ^{-1}. For a very large tree, the fluctuations of junctions in the central tier normalized by the mean-square end-to-end distance for long chains $\langle r_L^2\rangle_0$ in the undeformed state become

$$\frac{\langle(\Delta R)^2\rangle}{\langle r_L^2\rangle_0} = \frac{A}{A^2-1} = \frac{B}{B^2-\xi^{-2}} \tag{40}$$

In the derivation of eq 40, we used eqs 24, 25, 30, and 31. The double equality in eq 40 is in agreement with eq 37 relating A to B. For a unimodal network ($\xi = 1$), $A = B = \phi - 1$, and we rederive

$$\frac{\langle(\Delta R)^2\rangle}{\langle r^2\rangle_0} = \frac{\phi-1}{\phi(\phi-2)} \tag{41}$$

Since correlations of fluctuations of two junctions joined by a long chain are related to the nondiagonal elements of the inverse matrix given by eq 24, we have

$$\frac{\langle(\Delta\mathbf{R}_1\cdot\Delta\mathbf{R}_2)\rangle_L}{\langle r_L^2\rangle_0} = \frac{1}{A^2-1} \tag{42}$$

The subscript L in the quantity $\langle(\Delta\mathbf{R}_1\cdot\Delta\mathbf{R}_2)\rangle_L$ denotes that junctions 1 and 2 are connected by a long chain. Similarly, if $\langle(\Delta\mathbf{R}_1\cdot\Delta\mathbf{R}_2)\rangle_S$ denotes correlations of fluctuations of two junctions joined by a short chain, then from nondiagonal elements of the inverse matrix given by

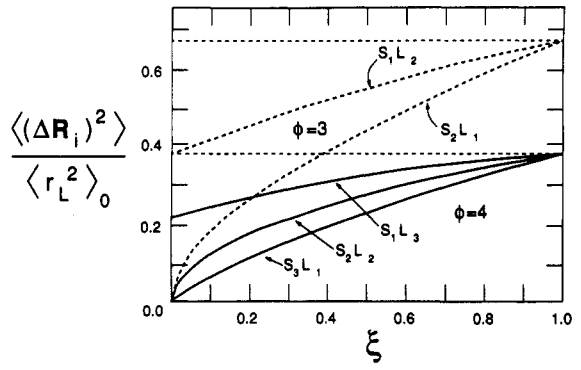

Figure 2. Mean-square fluctuations of junctions $\langle(\Delta R_i)^2\rangle / \langle r_i^2\rangle_0$ normalized by the mean-square end-to-end distance for long chains in various regular bimodal networks that are trifunctional (dashed lines) and tetrafunctional (solid lines) as a function of the ratio ξ of lengths of the short to long chains.

eq 25 it follows that

$$\frac{\langle(\Delta\mathbf{R}_1\cdot\Delta\mathbf{R}_2)\rangle_S}{\langle r_S^2\rangle_0} = \frac{1}{\xi^2 B^2 - 1} \tag{43}$$

For convenience, $\langle(\Delta\mathbf{R}_1\cdot\Delta\mathbf{R}_2)\rangle_L$ and $\langle(\Delta\mathbf{R}_1\cdot\Delta\mathbf{R}_2)\rangle_S$ are normalized by the mean-square end-to-end vectors in the undeformed state for long and short chains, respectively. For a unimodal network ($\xi = 1$), eqs 42 and 43 reduce to

$$\frac{\langle(\Delta\mathbf{R}_1\cdot\Delta\mathbf{R}_2)\rangle}{\langle r^2\rangle_0} = \frac{1}{\phi(\phi-1)} \tag{44}$$

Figure 2 shows the normalized fluctuations of junctions $\langle(\Delta\mathbf{R})^2\rangle / \langle r_L^2\rangle_0$ as a function of the ratio ξ ($0 < \xi < 1$) of the length of the short chains to the long ones. The solid lines in Figure 2 correspond to tetrafunctional networks, and the dashed lines correspond to trifunctional networks. The calculations have been performed for all possible regular bimodal networks with functionalities $\phi = 3$ and $\phi = 4$. In the following, we denote regular bimodal networks with i short chains and j long chains at each junction by S_iL_j.

As the ratio ξ of the lengths of short chains to long chains goes to 1, the normalized fluctuations of the junctions in trifunctional bimodal networks and in tetrafunctional bimodal networks approach the unimodal network fluctuations $(\phi - 1)/[\phi(\phi - 2)]$, i.e., $^3/_8$ for a tetrafunctional network and $^2/_3$ for a trifunctional network. The behavior of the fluctuations in the limit $\xi \to 0$, when the short chains become infinitely short in comparison with the long ones, is very interesting. For a regular bimodal S_1L_2 or S_1L_3 network, normalized fluctuations of junctions in the limit $\xi \to 0$ approach 0.2083 for $\phi = 4$ and 0.375 for $\phi = 3$. For a regular bimodal network with junctions connected to at least two short chains, the normalized fluctuations of junctions in the limit $\xi \to 0$ go to 0. The explanation of this behavior is very simple. In the limit $\xi \to 0$, short chains reduce to points and a bifunctional trifunctional network with treelike topology and $\phi_S = 1$ becomes a unimodal tetrafunctional treelike network. Therefore, its normalized fluctuations become $^3/_8 = 0.375$. Similarly, a bimodal tetrafunctional network with $\phi_S = 1$ and in the limit $\xi \to 0$ becomes a unimodal hexafunctional network with treelike topology, and normalized fluctuations of junctions in a unimodal hexafunctional network are exactly $^5/_{24} \approx 0.2083$. In the case where the number of short chains at the junctions exceeds 1 ($\phi_S > 1$), the bimodal network with treelike structure in the limit $\xi \to 0$ becomes a unimodal network with infinite functionality, and therefore, the fluctuations of the junctions go to 0. Figure 2 shows

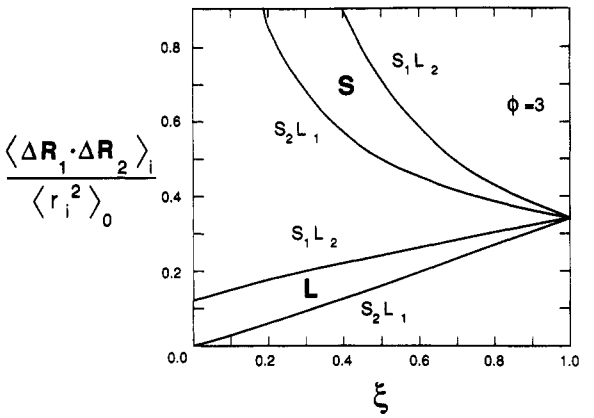

Figure 3. Correlations of fluctuations of two junctions $\langle\Delta\mathbf{R}_1\cdot\Delta\mathbf{R}_2\rangle_i / \langle r_i^2\rangle_0$ (i = S, L) connected by a short or long chain, normalized by mean-square end-to-end distance of the chain connecting the junctions, shown as a function of the ratio ξ of the lengths of short to long chains for various regular bimodal networks that are trifunctional.

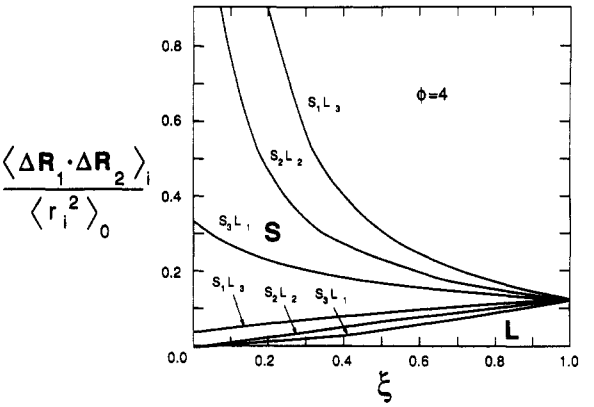

Figure 4. Correlations of fluctuations of two junctions $\langle\Delta\mathbf{R}_1\cdot\Delta\mathbf{R}_2\rangle_i / \langle r_i^2\rangle_0$ (i = S, L) connected by a short or long chain, normalized by mean-square end-to-end distance of the chain connecting the junctions, shown as a function of the ratio ξ of the lengths of short to long chains for various regular bimodal networks that are tetrafunctional.

also that for a given value ξ of the ratio of the lengths of the short chains to those of the long chains and for a given functionality the normalized fluctuations of the junctions increase as the number of long chains ϕ_L connected with the junctions increases.

Figures 3 and 4 show correlations of fluctuations $\langle(\Delta\mathbf{R}_1\cdot\Delta\mathbf{R}_2)\rangle_i / \langle r_i^2\rangle_0$ of two junctions 1 and 2 connected by a short chain (i = S) or by a long chain (i = L) normalized by the mean-square end-to-end distance in the undeformed state of a chain connecting these junctions. Figure 3 shows the relevant correlations for two different regular bimodal trifunctional networks, specifically S_1L_2 and S_2L_1, as a function of the ratio ξ. Figure 4 shows the same for three different regular bimodal tetrafunctional networks, specifically S_1L_3, S_2L_2, and S_3L_1. The letter L denotes plots showing correlations of fluctuations of junctions connected by a long chain and the letter S correlations of junctions connected by a short chain. The characteristic feature of both figures is that normalized correlations of fluctuations of junctions connected by a long chain are always finite in the limit $\xi \to 0$, whereas normalized correlations of junctions connected by short chains may become infinite in this limit. More specifically, the correlations of fluctuations of junctions connected by a long chain in the limit $\xi \to 0$ go to 0 for trifunctional bimodal S_2L_1 networks and to 0.125 for S_1L_2. For tetrafunctional bimodal networks, these correlations approach 0 in the limit $\xi \to$

0 for S_3L_1 and S_2L_2, while for S_1L_3 for $\xi \to 0$ they become 0.041 67. In the limit $\xi \to 0$, a bimodal trifunctional S_1L_2 network becomes effectively a unimodal tetrafunctional network composed of long chains and the tetrafunctional S_1L_3 network becomes a unimodal hexafunctional network with normalized correlations $1/[\phi(\phi - 2)] = 0.125$ and 0.041 67, respectively. If the number of short chains attached to junctions exceeds 1 ($\phi_S > 1$), then in the limit $\xi \to 0$ both tetrafunctional and trifunctional bimodal networks become effectively unimodal networks composed of long chains and the infinite functionalities and correlations of fluctuations of junctions vanish. The normalized correlations of fluctuations of junctions connected by a short chain go to infinity in the limit $\xi \to 0$ for S_1L_2, S_2L_1, S_2L_2, and S_1L_3. For a S_3L_1 network, the normalized correlations of junctions connected by a short chain are finite for $\xi = 0$ and are equal to 0.333. This also has a simple explanation. A bimodal network (both for $\phi = 3$ and for $\phi = 4$) having only one short chain at each junction ($\phi_S = 1$) behaves in the limit $\xi \to 0$ as a collection of free ($\phi = 0$) short chains, because infinitely long chains connected with short ones do not restrict the motion of short chains and may be neglected. Similarly, a bimodal network with two short chains attached to each junction ($\phi_S = 2$) behaves in the limit $\xi \to 0$ as a system of infinitely long bifunctional chains ($\phi = 2$) composed of short chains, if the long chains that do not restrict the motion of short ones are neglected. In both these cases, $\phi = 0$ and $\phi = 2$, the normalized correlations according to the formula $1/[\phi(\phi - 2)]$ become infinite. We should note that if these correlations are normalized by the mean square-end-to-end vector for long chains $\langle r_L^2 \rangle$ instead of by $\langle r_S^2 \rangle$, then $\langle (\Delta \mathbf{R}_1 \cdot \Delta \mathbf{R}_2)_S / \langle r_L^2 \rangle$ is finite in the limit $\xi \to 0$. The tetrafunctional S_3L_1 network in the limit $\xi \to 0$ becomes a trifunctional unimodal network composed of short chains, if infinitely long chains are neglected, and therefore the normalized correlations of fluctuations of junctions connected by short chain are finite and equal to $^1/_3$. The normalized correlations plotted in Figures 3 and 4 in the limit $\xi = 1$ approach the corresponding values for unimodal networks, namely $^1/_3$ for $\phi = 3$ (Figure 3) and $^1/_8$ for $\phi = 4$ (Figure 4). With increasing number of long chains in the network, the normalized correlations in Figures 3 and 4 increase both for junctions connected by a short chain and by a long one.

Knowledge of the fluctuations of junctions in bimodal networks and correlations among them enables one to calculate the squared fluctuations of the end-to-end vectors $\langle (\Delta r_S)^2 \rangle$ for short chains and $\langle (\Delta r_L)^2 \rangle$ for long chains. By using eqs 9 and 40–43, the relative fluctuations of end-to-end vectors are seen to be given by

$$\frac{\langle (\Delta r_S)^2 \rangle}{\langle r_S^2 \rangle_0} = \frac{2}{B\xi + 1} \tag{45}$$

and

$$\frac{\langle (\Delta r_L)^2 \rangle}{\langle r_L^2 \rangle_0} = \frac{2}{A + 1} \tag{46}$$

for short and long chains, respectively, where A and B are solutions of the double recurrence (eq 35). For the unimodal network ($\xi = 1$, $A = B = \phi - 1$), eqs 45 and 46 reduce to the known formula

$$\langle (\Delta r)^2 \rangle = \frac{2}{\phi} \langle r^2 \rangle_0 \tag{47}$$

Figure 5 shows the dependence of relative fluctuations $\langle (\Delta r)_i^2 \rangle / \langle r_i^2 \rangle_0$ for short chains (i = S) and long chains (i = L) as a function of the ratio ξ of lengths of short to long chains for different regular bimodal networks that are trifunctional. The same information for regular bimodal networks that are tetrafunctional is shown in Figure 6. The upper parts of Figures 5 and 6 show the relative fluctuations of the mean-square end-to-end vectors for short chains (denoted by a letter S), and lower parts of these figures show these fluctuations for long chains (denoted by a letter L). For $\xi \to 1$, all curves in Figures 5 and 6 converge to the values $2/\phi$ for fluctuations in unimodal networks, i.e., to $^2/_3$ for trifunctional networks (Figure 5) and $^1/_2$ for tetrafunctional ones (Figure 6). The relative fluctuations of short chains are always greater than the corresponding fluctuations in the unimodal network with the same functionality, while relative fluctuations of long chains are always less then fluctuations in this unimodal network. In the limit $\xi \to 0$, the fluctuations of the mean-square end-to-end distance for long chains go to zero if the number of short chains attached to each junction exceeds one, as seen for the S_2L_1 networks shown in Figure 5 and for S_3L_1 and S_2L_2 networks in Figure 6. If each junction in the network is attached to only one short chain ($\phi_S = 1$), then the relative fluctuations of the mean-square end-to-end distance of the long chains in the limit $\xi \to 0$ go to either $^1/_2$ (for S_1L_2) or to $^1/_3$ (for S_1L_3). This can easily be explained since in the first case ($\phi_S > 1$) a bimodal network becomes effectively a unimodal one

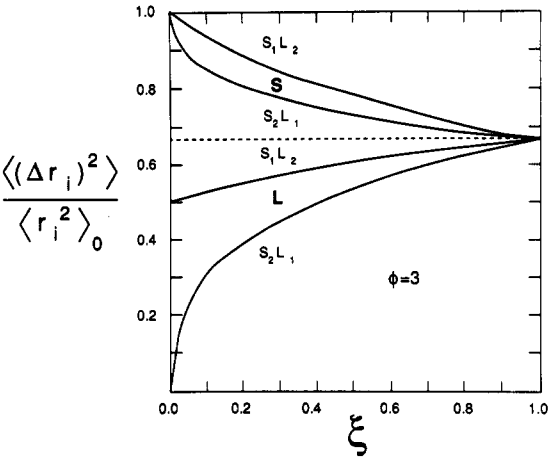

Figure 5. Relative mean-square fluctuations $\langle (\Delta r_i)^2 \rangle / \langle r_i^2 \rangle_0$ of the end-to-end vectors for short and long chains (i = S, L) as a function of the ratio ξ of lengths of short to long chains for various regular bimodal networks that are trifunctional.

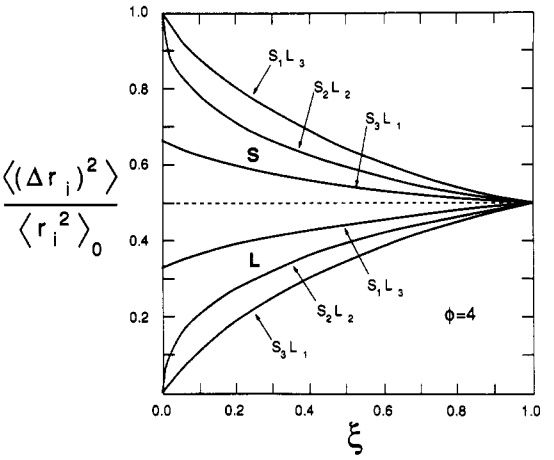

Figure 6. Relative mean-square fluctuations $\langle (\Delta r_i)^2 \rangle / \langle r_i^2 \rangle_0$ of the end-to-end vectors for short and long chains (i = S, L) as a function of the ratio ξ of lengths of short to long chains for various regular bimodal networks that are tetrafunctional.

composed of long chains with infinite functionality and therefore chain fluctuations go to zero. For $\phi_S = 1$, the trifunctional bimodal network becomes effectively a tetrafunctional unimodal network composed of long chains and the tetrafunctional bifunctional network becomes a hexafunctional unimodal one. Since the relative fluctuations of the mean-square end-to-end vectors in unimodal networks are $2/\phi$, we obtain the values $^1/_2$ and $^1/_3$ for the S_1L_2 and S_1L_3 networks, respectively. The relative fluctuations of the mean-square end-to-end distance for short chains in bimodal networks in the limit $\xi \to 0$ go to unity if the number of short chains connected to each junction is one ($\phi_S = 1$) or two ($\phi_S = 2$) as seen in Figure 5 for S_1L_2 and S_2L_1 networks and in Figure 6 for S_1L_3 and S_2L_2 networks. If the number of short chains attached to each junction is $\phi_S = 3$ as in the S_3L_1 bimodal network (Figure 6), then the relative fluctuations for short chains in the limit $\xi \to 0$ are $^2/_3$. The explanation is similar to that given above. If the long chains are infinitely long in comparison with the short chains, the connectivity of long chains with short ones may be neglected when studying the behavior of the short chains. Therefore, for $\phi_S = 1$ and $\phi_S = 2$, the network is equivalent to the system of free short chains (if $\phi_S = 1$) or infinitely long bifunctional networks (chains) composed of short chains (if $\phi_S = 2$). In both cases, mean end-to-end vectors are zero and therefore the mean-square fluctuations of the end-to-end vector for short chains are equal to the mean-square end-to-end vectors themselves, i.e., $\langle(\Delta r_i)^2\rangle/\langle r_i^2\rangle_0 = 1$. In the case of an S_3L_1 network in the limit $\xi \to 0$, neglecting the long chains causes the network to become a unimodal trifunctional one composed of short chains with relative fluctuations of short chains given by $2/\phi$, i.e., by $^2/_3$. Figures 5 and 6 show that, for a given functionality, an increase in the number of short chains connected to each junction decreases the relative fluctuations of both long and short chains.

Such fluctuations of chain end-to-end distances in networks can be measured experimentally by SANS. In the following section we derive expressions for small-angle neutron scattering factors for scattering from regular bimodal networks.

Small-Angle Neutron Scattering from Regular Bimodal Networks

Small-angle neutron scattering studies of elastomeric networks have recently become a rapidly growing field of polymer science.[12-14] Recent progress in this experimental technique enables one to study structure and dynamics of polymer chains in networks in both the undeformed and stretched states at the molecular level. The power and versatility of SANS permits the critical assessment of the various molecular theories of rubber elasticity.

In order to study chains by using neutron scattering, labeled (deuterated) chains are incorporated into normal, nondeuterated networks. Such labeled chains may be end linked into the network or may be randomly cross-linked into it; the scattering form factor for end-linked chains differs from that for the cross-linked ones.

The problem of small-angle neutron scattering from labeled end-linked chains in a unimodal (monodisperse) phantom Gaussian network with treelike topology was first studied by Pearson.[8] Recently, an alternative phantom network model has been proposed and results calculated from it compared with experimental data.[15] Neutron scattering from labeled chains cross-linked into the network has been studied first by Warner and Edwards[16] using the replica model and later by Ullman,[17] Higgs and Ball,[10] and Kloczkowski et al.[18] using the exact solution of the James-Guth model[2] for unimodal networks with treelike topologies. The problem of neutron scattering from polydisperse networks has been first studied by Higgs and Ball by using a resistor network method.[10]

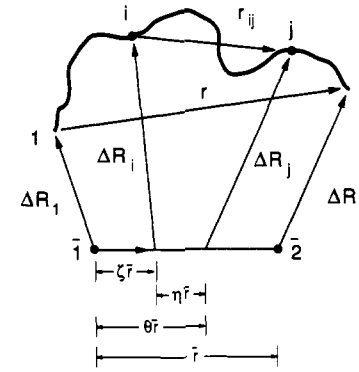

Figure 7. Instantaneous configuration of a typical chain in a phantom network.

The scattering form factor from the labeled chains in the network is given by the Fourier transform of the distribution function $\Omega(\mathbf{r}_{ij})$ of distances $\mathbf{r}_{ij}$ between scattering centers i and j on the chain. Specifically,

$$S(\mathbf{q}) = \frac{1}{N^2}\sum_{i,j=1}^{N}\int \exp(i\mathbf{q}\cdot\mathbf{r}_{ij})\,\Omega(\mathbf{r}_{ij})\,d\mathbf{r}_{ij} \tag{48}$$

where N is the number of scattering centers along the chain length. The Gaussian distribution function $\Omega(\mathbf{r}_{ij})$ of the vector $\mathbf{r}_{ij}$ in the deformed state is

$$\Omega(\mathbf{r}_{ij}) = [(2\pi)^3\langle x_{ij}^2\rangle\langle y_{ij}^2\rangle\langle z_{ij}^2\rangle]^{-1/2} \times \exp\left[-\frac{x_{ij}^2}{2\langle x_{ij}^2\rangle} - \frac{y_{ij}^2}{2\langle y_{ij}^2\rangle} - \frac{z_{ij}^2}{2\langle z_{ij}^2\rangle}\right] \tag{49}$$

where $\langle x_{ij}^2\rangle$, $\langle y_{ij}^2\rangle$, and $\langle z_{ij}^2\rangle$ are the mean-square components of the vector $\mathbf{r}_{ij}$ in the deformed state. Substitution of the expression for $\Omega(\mathbf{r}_{ij})$ from eq 49 into eq 48 leads to

$$S(\mathbf{q}) = \frac{1}{N^2}\sum_{i,j=1}^{N}\exp[-q_x^2\langle x_{ij}^2\rangle/2 - q_y^2\langle y_{ij}^2\rangle/2 - q_z^2\langle z_{ij}^2\rangle/2] \tag{50}$$

where q_x, q_y, and q_z are components of the scattering vector $\mathbf{q}$ representing the difference between the incident and scattered wave vectors $\mathbf{k}_0$ and $\mathbf{k}$. The length of the scattering vector q is related to the scattering angle ϑ by

$$q = \frac{4\pi}{\lambda}\sin(\vartheta/2) \tag{51}$$

where λ is the wavelength of the radiation.

Figure 7 shows the instantaneous configuration of a typical chain in a phantom network. Points 1 and 2 denote the ends of the chain at a given instant and $\bar{1}$ and $\bar{2}$ the mean positions of junctions 1 and 2. The instantaneous end-to-end vector is denoted by $\mathbf{r}$, and $\bar{\mathbf{r}}$ is the time-averaged end-to-end vector. Here $\Delta\mathbf{R}_1$ and $\Delta\mathbf{R}_2$ are the instantaneous fluctuations of junctions 1 and 2 from their mean positions. The instantaneous fluctuations of two points i and j on the chain from their mean positions are $\Delta\mathbf{R}_i$ and $\Delta\mathbf{R}_j$. We assume that the chain is freely jointed and fractional distances of points i and j from junction 1 are ζ and θ, respectively. The fractional distance between two points on the chain is defined as a ratio of the contour length of the chain between these points to the total

contour length of the chain. The fractional distance between points i and j is $\eta = |\zeta - \theta|$. It may be shown that fluctuations $\langle(\Delta r_{ij})^2\rangle_0$ of the vector $\mathbf{r}_{ij}$ between points i and j are related to the fluctuations $\langle(\Delta r)^2\rangle_0$ of the end-to-end vector of the chain in the undeformed state by[9]

$$\langle(\Delta r_{ij})^2\rangle = \langle(\Delta R_i)^2\rangle + \langle(\Delta R_j)^2\rangle - 2\langle\Delta\mathbf{R}_i\cdot\Delta\mathbf{R}_j\rangle = \eta(1-\eta)\langle r^2\rangle_0 + \eta^2\langle(\Delta r)^2\rangle_0 \quad (52)$$

Assuming that fluctuations are strain independent and that mean distances transform affinely with strain, we obtain

$$\langle x_{ij}^2\rangle = \lambda_x^2\langle\bar{x}_{ij}\rangle_0 + \langle(\Delta x_{ij})^2\rangle = \lambda_x^2\langle r_{ij}^2\rangle_0/3 + (1-\lambda_x^2)\langle(\Delta r_{ij})^2\rangle_0/3 \quad (53)$$

with similar equations for $\langle y_{ij}^2\rangle$ and $\langle z_{ij}^2\rangle$. Using eq 52 and the assumption that the chains are freely jointed,

$$\langle r_{ij}^2\rangle_0 = \eta\langle r^2\rangle_0 \quad (54)$$

leads to

$$\langle x_{ij}^2\rangle = \left[\lambda_x^2 + (1-\lambda_x^2)\left(1 - \eta + \eta\frac{\langle(\Delta r)^2\rangle}{\langle r^2\rangle_0}\right)\right]\eta\langle r^2\rangle_0/3 \quad (55)$$

Substituting eq 55 into eq 50, replacing double summations by integrals $\int_0^1 d\xi \int_0^1 d\theta$, and performing one of these integrations lead finally to the following expression for the scattering form factor in the direction parallel to the direction of stretch (identified with the x direction)

$$S_\parallel(q) = 2\int_0^1 d\eta\,(1-\eta)\times \exp\left\{-\nu\left[\lambda_\parallel^2\eta + (1-\lambda_\parallel^2)\left(\eta - \eta^2 + \eta^2\frac{\langle(\Delta r)^2\rangle}{\langle r^2\rangle_0}\right)\right]\right\} \quad (56)$$

In this equation

$$\nu = q^2\langle r^2\rangle_0/6 \quad (57)$$

and $\lambda_\parallel$ is the component of the deformation gradient tensor in the direction parallel to stretch. The scattering form factor for the scattering in the direction perpendicular to the direction of stretch is obtained by replacing $\lambda_\parallel$ in eq 56 by $\lambda_\perp = 1/\sqrt{\lambda_\parallel}$.

If short chains in the regular bimodal network are labeled, then the scattering form factor for short chains is obtained from eq 56 with $\langle r^2\rangle_0 = \langle r_S^2\rangle_0$ by replacing $\langle(\Delta r_S)^2\rangle/\langle r_S^2\rangle_0$ by the right-hand side of eq 45 and then solving the double recurrence (eq 35) for B. If long chains in the regular bimodal network are labeled, the corresponding scattering form factor is obtained from eq 56 with $\langle r^2\rangle_0 = \langle r_L^2\rangle_0$ and relative fluctuations of long chains $\langle(\Delta r_L)^2\rangle/\langle r_L^2\rangle_0$ given by eq 46. It should be noted that the scattering form factor $S(q)$ in eq 56 has been derived for labeled chains end-linked into the network. Thus, there are no cross-links (except two terminal ones) along the labeled chains. The scattering form factor from a labeled chain cross-linked into the bimodal network would differ.

In the limiting case of a unimodal network, eq 56 reduces to the Pearson result.[8] Figure 8 shows Kratky plots [$\nu S_\parallel(q)$ vs ν] for scattering from labeled short and long chains in the direction parallel to stretch in various regular bimodal trifunctional networks. Figure 9 shows similar Kratky plots for various bimodal tetrafunctional networks. The results have been obtained for bimodal networks with the ratio of lengths of short and long chains given by $\xi = 0.1$ and for the extension ratio $\lambda = 2$. Solid lines in Figures 8 and 9 show scattering from long chains and dashed lines from short chains. The upper solid lines in both figures show scattering from undeformed networks ($\lambda = 1$). In the undeformed networks, both short and long chains have the same scattering form factor

$$S(q) = \frac{2}{\nu^2}(e^{-\nu} + \nu - 1) \quad (58)$$

corresponding to the scattering from an unperturbed Gaussian coil, irrespective of the number of short and long chains attached to each junction. All remaining curves refer to the deformed ($\lambda = 2$) networks. With increasing the number of short chains attached to each junction in the regular bimodal network, the scattering form factors from both long labeled chains and short labeled chains decrease. The unimodal networks composed of either long or short chains (L_3 and S_3 in Figure 8 and L_4 and S_4 in Figure 9) have the same scattering form factors, shown by the first solid line below the dashed ones. As the extension ratio λ increases, scattering form factors for the scattering parallel to deformation from both short and long labeled chains decrease, as in the unimodal networks. With increasing values of the ratio ξ of the length of short chains to long chains, form factors for scattering parallel to the stretch direction increase for short chains but decrease for long chains. Form factors $S_\perp$ for scattering perpendicular to the direction of stretch (not shown in Figures 8 and 9) are always larger than the form factor for unstretched networks. Form factors for short chains are smaller than those for long chains, and the difference increases as λ decreases. As the number of short chains attached to each junction in the regular bimodal network increases, the form factors $S_\perp$ for scattering from long

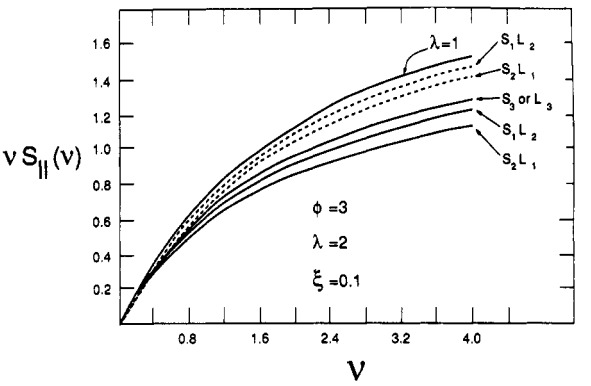

Figure 8. Kratky plots [$\nu S_\parallel(\nu)$ vs ν] for neutron scattering in the direction parallel to stretch ($\lambda = 2$, $\xi = 0.1$) from labeled short chains (dashed lines) and long chains (solid lines) for various regular bimodal networks that are trifunctional.

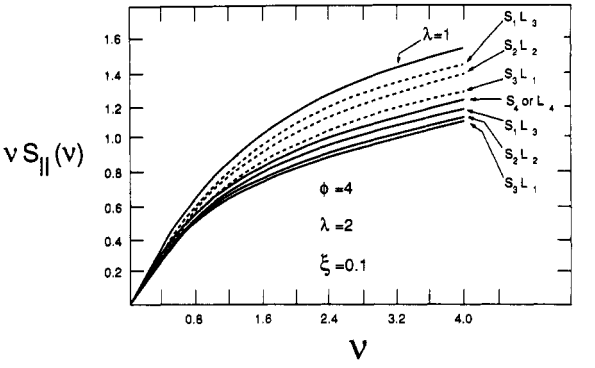

Figure 9. Kratky plots [$\nu S_\parallel(\nu)$ vs ν] for neutron scattering in the direction parallel to stretch ($\lambda = 2$, $\xi = 0.1$) from labeled short chains (dashed lines) and long chains (solid lines) for various regular bimodal networks that are tetrafunctional.

and short chains increase (opposite to the decrease shown by $S_{\parallel}$). With increasing values of the ratio ξ, scattering form factors $S_{\perp}$ for scattering perpendicular to the direction of stretch increase for long chains but decrease for short chains. The Kratky plots for scattering from labeled end-linked chains in directions both parallel and perpendicular to the direction of stretch are monotonically increasing functions of ν. If the labeled chains in the bimodal network are crosslinked, we may expect maxima in the Kratky plots of $\nu S_{\perp}(\nu)$ similar to those obtained for unimodal networks.

Discussion

The results presented in this paper have been calculated for phantom Gaussian bimodal regular networks with the topology of an infinite tree. The regularity of the network refers to the requirement that each junction in the network is connected to the same number ϕ_S of short chains and the same number ϕ_L of long chains. Recently Sharaf and Mark[11] synthesized regular bimodal trifunctional networks with each junction connected with one short and two long chains ($\phi_S = 1, \phi_L = 2$). Synthesis of other types of regular bimodal networks is currently under way.

A theory of randomly cross-linked bimodal networks has been developed recently by Higgs and Ball.[10] The exact solution of the problem obtained by Higgs and Ball requires the solution of a nonlinear integral equation by iterative methods. They also presented a simple mean-field solution to the problem for bimodal networks. If the mole fractions of short and long chains in random bimodal network are x_S and x_L, respectively, and the ratio of lengths of short to long chains is ξ, then the fluctuations of the mean-square end-to-end vectors for short and long chains according to the Higgs and Ball mean-field theory are

$$\frac{\langle(\Delta r_S)^2\rangle}{\langle r_S^2\rangle_0} = \frac{2Y}{2Y+\xi} \tag{59}$$

and

$$\frac{\langle(\Delta r_L)^2\rangle}{\langle r_L^2\rangle_0} = \frac{2Y}{2Y+1} \tag{60}$$

with Y (X_M/S_L in Higgs and Ball notation) given by

$$Y = [1+\xi-(\phi-1)(x_L\xi+x_S)+ \sqrt{[(\phi-1)(x_L\xi+x_S)-(1+\xi)]^2+4(\phi-2)\xi}]/[2(\phi-2)] \tag{61}$$

where ϕ is the network functionality. Higgs and Ball proved also that the exact value of the variable Y (obtained by solving an integral equation) is always larger than the value obtained from eq 61 using the mean-field approximation. It means that exact predictions of the fluctuations of the end-to-end distance for both short and long chains in random bimodal networks are always larger than the fluctuations calculated from the mean-field theory. The mean-field theory of Higgs and Ball gives very good agreement with the exact solution, however, if the difference in lengths between short and long chains is relatively small. The difference between the exact and the mean field solutions grows rapidly as $\xi \to 0$. Figure 10 shows the relative fluctuations of the end-to-end distance for short chains $\langle(\Delta r_S)^2\rangle/\langle r_S^2\rangle_0$ (upper part of Figure 10) and for long chains $\langle(\Delta r_L)^2\rangle/\langle r_L^2\rangle_0$ (lower part of Figure 10) as a function of the ratio of the lengths of short and long chains in bimodal tetrafunctional networks. Solid lines correspond to relative fluctuations in regular

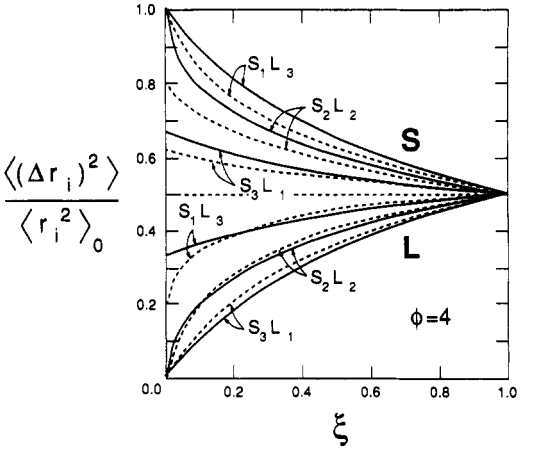

Figure 10. Comparison of relative fluctuations $\langle\Delta r_i\rangle^2/\langle r_i^2\rangle_0$ of short (i = S) and long chains (i = L) for various regular bimodal networks that are tetrafunctional (solid lines) with results based on the Higgs and Ball mean-field theory (dashed lines).

bimodal networks and dashed lines in random bimodal networks composed of the same fractions of short and long chains as in regular networks, i.e., with $x_S/x_L = \phi_S/\phi_L$. The relative fluctuations of the end-to-end vectors for short chains in random bimodal networks calculated by using the mean-field approximation are always smaller than fluctuations in regular bimodal networks. The relative fluctuations of the end-to-end distance for long chains in random bimodal network with $x_S = 0.75$ and $x_L = 0.25$ according to mean-field theory are larger than fluctuations in regular S_3L_1 networks, irrespective of ξ. The relative fluctuations of the end-to-end vector for long chains in random bimodal networks with $x_S = x_L = 0.5$ and $x_S = 0.25$, $x_L = 0.75$ in the mean-field approximation are either larger (for large ξ) or smaller (for small ξ) than fluctuations in the corresponding regular S_2L_2 and S_1L_3 networks.

The exact solution of the regular bimodal network model satisfies the relation

$$x_S\frac{\langle(\Delta r_S)^2\rangle}{\langle r_S^2\rangle_0} + x_L\frac{\langle(\Delta r_L)^2\rangle}{\langle r_L^2\rangle_0} = 2/\phi \tag{62}$$

which may be written as

$$\frac{\phi_S}{B\xi+1} + \frac{\phi_L}{A+1} = 1 \tag{63}$$

The expression given by eq 63 may be analytically proved by substituting A calculated from eq 63 into eq 36a. The resulting quartic equation for B differs from eq 38, but after division by $B+\xi^{-1}$, one obtains eq 39. This confirms that the front factor $g = 1 - 2/\phi$ for regular bimodal networks depends only on the functionality of the network and is the same as that for random networks, thus supporting the results obtained by Graessley.[5,6]

Throughout the paper we assumed that chains are Gaussian. For real bimodal networks, the non-Gaussian behavior of the short chains plays an important role, improving the ultimate properties of networks.[19] The present theory assumes also that chains are phantom, whereas real bimodal networks are not phantom because of entanglements and steric effects. A more realistic theory of bimodal networks must take into account both of these effects. However, the phantom Gaussian theory as a first approximation is a good starting point for more realistic theories of bimodal networks.

Acknowledgment. It is a pleasure to acknowledge the financial support provided J.E.M. by the National Science Foundation through Grant DMR 89-18002 (Polymers Program, Division of Materials Research).

References and Notes

(1) James, H. M. *J. Chem. Phys.* **1947**, *15*, 651.
(2) James, H. M.; Guth, E. *J. Chem. Phys.* **1947**, *15*, 669.
(3) Duiser, J. A.; Staverman, A. J. In *Physics of Non-Crystalline Solids*; Prins, J. A., Ed.; North-Holland: Amsterdam, 1965.
(4) Eichinger, B. E. *Macromolecules* **1972**, *5*, 496.
(5) Graessley, W. W. *Macromolecules* **1975**, *8*, 186.
(6) Graessley, W. W. *Macromolecules* **1975**, *8*, 865.
(7) Flory, P. J. *Proc. R. Soc. London, Ser. A* **1976**, *351*, 351.
(8) Pearson, D. S. *Macromolecules* **1977**, *10*, 696.
(9) Kloczkowski, A.; Mark, J. E.; Erman, B. *Macromolecules* **1989**, *22*, 1423.
(10) Higgs, P. G.; Ball, R. C. *J. Phys. (Fr.)* **1988**, *49*, 1785.
(11) Sharaf, M. A.; Mark, J. E. *Macromol. Rep.* **1991**, *1*, 67.
(12) Picot, C. *Prog. Colloid Polym. Sci.* **1987**, *75*, 83.
(13) Bastide, J.; Herz, J.; Boué, F. *J. Phys. (Fr.)* **1985**, *46*, 1967.
(14) Boué, F. *Adv. Polym. Sci.* **1987**, *82*, 1.
(15) Kloczkowski, A.; Mark, J. E.; Erman, B. *Macromolecules* **1990**, *23*, 1222.
(16) Warner, M.; Edwards, S. F. *J. Phys. A. Math. Gen.* **1978**, *11*, 1649.
(17) Ullman, R. *Macromolecules* **1982**, *15*, 1395.
(18) Kloczkowski, A.; Mark, J. E.; Erman, B. *Macromolecules* **1989**, *22*, 4502.
(19) Mark, J. E.; Erman, B. *Rubberlike Elasticity. A Molecular Primer*; Wiley-Interscience: New York, 1988.